Annals of Communications in Mathematics
Volume 9, Number 2 (2026), 15
DOI: 10.62072/acm.2026.09031
ISSN: 2582-0818
https://www.technoskypub.com/journal/acm/

Research article

The Power Reduced Kies Distribution: Theory and Applications in Environmental, Insurance, and Health Sciences

Ehinomen Emmanuel Ehizojie *

Department of Statistics, Ahmadu Bello University, Nigeria.

*Corresponding Author: Ehinomen Emmanuel Ehizojie. Email: ehizojieee@gmail.com
Received: 17 May 2026; Accepted: 18 June 2026; Published: 30 June 2026

Citation: E. E. Ehizojie, The Power Reduced Kies Distribution: Theory and Applications in Environmental, Insurance, and Health Sciences. Ann. Commun. Math. 9 **(2026)**, 15. https://doi.org/10.62072/acm.2026.09031

Abstract: The adequacy of a statistical model ultimately rests on how faithfully the chosen distribution captures the structural features of the data at hand, including skewness, kurtosis, multi-modality, and the shape of the HRF. Consequently, the construction of new and more flexible distributions remains an active and consequential area of statistical research. In the same vein, this study introduces the Power Reduced Kies distribution (PRKD), a new two-parameter bounded distribution obtained through the power transformation of random variable of the Reduced Kies distribution. The inclusion of the power parameter endows the PRKD with a substantially richer variety of density shapes, including decreasing, right-skewed, left-skewed, reversed-J, and approximately symmetric forms, as well as a wider range of hazard rate behaviours, including increasing and bathtub-shaped forms, none of which can be collectively achieved by the single-parameter Reduced Kies distribution. Several important statistical properties of the PRKD are derived, including its linear representation, reliability characteristics, quantile function, moments, moment generating function, mode, and order statistics. The model parameters are estimated using the maximum likelihood and maximum product of spacings methods. A Monte Carlo simulation study is conducted to examine the finite-sample performance of the estimators under different parameter settings and sample sizes using mean estimates and mean squared errors. The results indicate that both estimators perform satisfactorily, although the maximum product of spacings method generally provides more reliable estimates for smaller sample sizes. The practical applicability of the PRKD is demonstrated using four real datasets from environmental, insurance, and health sciences. Comparative analyses with twelve competing unit distributions reveal that the PRKD provides highly competitive fits according to several model selection criteria and goodness-of-fit measures.

Mathematics Subject Classification: 60E05, 62E15, 62F10, 62P99
Keywords: Reduced Kies distribution; power transformation, moments, reliability characteristics, unit distributions

1 Introduction

Probability distribution theory remains a fundamental pillar of statistical science, providing the necessary mathematical structure to characterise the randomness inherent in empirical phenomena. Historically, the pursuit of more versatile models has been driven by the need to capture complex data structures that traditional models fail to accommodate. By extending existing families of distributions or developing novel generators, researchers can improve the goodness-of-fit and predictive accuracy of statistical inferences across diverse scientific domains.

While a plethora of probability distributions has been proposed to interpret real-world phenomena, the majority are defined on the positive real line or the entire real line. In numerous applied disciplines, however, data are naturally confined to bounded intervals. Proportions, rates, indices, and standardised scores arising in economics, medicine, biology, environmental studies, and quality control typically lie within $(0, 1)$ or other finite ranges after appropriate transformation. Employing unbounded distributions for such data can produce unrealistic probability assignments beyond the support and yield biased parameter estimates or predictions. Bounded distributions, especially those defined on the unit interval $(0, 1)$, therefore hold considerable practical value, as a linear transformation readily extends them to any desired bounded interval.

Although bounded data occur frequently in practice, the statistical literature has historically provided fewer models with bounded support than the extensive collection available for unbounded domains. The beta distribution, first examined by [7] and popularised by Karl Pearson as the Pearson type I distribution, remains the most extensively used model for unit-interval data. Later classical contributions include the Topp-Leone distribution [32] and the Kumaraswamy distribution [23]. It is clear there is a sparseness of bounded models in the past century but, fortunately, in recent decades researchers have shown renewed interest in developing flexible bounded distributions capable of accommodating varied shapes, skewness levels, and tail behaviours encountered in empirical datasets.

Recent literature has witnessed the development of several unit distributions. For instance, [20] introduced the unit log-log distribution, [13] proposed the unit exponential Pareto distribution, [6] introduced the Bounded Exponentiated Weibull distribution, [30] developed the Unit Logistic Exponential Distribution, and [33] proposed the log-inverse Gompertz distribution, among others.

The baseline distribution chosen for this work is the Reduced Kies distribution (RKD), first introduced by [21], derived from the Kies distribution [18] by restricting its support to the unit interval. The RKD is a single-parameter distribution with support on the unit interval $(0, 1)$, making it a natural candidate for modelling bounded data. The uniqueness of the RKD lies in its extremely simple mathematical form and its connection to the exponential distribution through a reciprocal transformation. However, the RKD suffers from a lack of flexibility because it has only one parameter, which cannot capture varying skewness and kurtosis. Recognising these limitations, several researchers have proposed extensions and generalisations of the RKD to enhance its flexibility. Recent examples include the extended Reduced Kies distribution by [3], Marshall-Olkin Reduced Kies by [2], Kumaraswamy Reduced Kies distribution by [14], exponentiated generalised Reduced Kies distribution [9], and the alpha power Reduced Kies distribution [10].

Motivated by these considerations, this study proposes a novel generalisation of the RKD via a power transformation technique, resulting in a new two-parameter model termed the Power Reduced Kies distribution (PRKD). The power transformation involves taking $Y = X^{1/\alpha}$ or equivalently $X = Y^{\alpha}$ for $\alpha > 0$, which generates a new distribution with one additional shape parameter. This technique has been widely used in distribution theory to improve flexibility and tail behaviour of existing models. Recent examples include the power transmuted inverse Rayleigh distribution by [16], the power Burr Type X distribution by [34], the power inverse Gompertz distribution by [1], the power unit Burr-XII distribution by [35], the power inverse Lomax distribution by [15], the power unit inverse Lindley distribution by [11], the power unit exponential probability distribution by [4], the power modified XLindley distribution by [31], the power new XLindley distribution by [12], and the power odd Lindley half-logistic distribution by [17], among others. These studies demonstrate the effectiveness of power transformations in generating flexible distributions capable of modelling diverse data behaviours.

The proposed PRKD offers several distinctive advantages over existing generalisations of the RKD and over classical unit distributions more broadly. First, the inclusion of the power parameter endows the PRKD with a substantially richer variety of density shapes, including decreasing, right-skewed, left-skewed, reversed-J, and approximately symmetric forms, as well as a wider range of hazard rate behaviours, including increasing and bathtub-shaped forms, none of which can be collectively achieved by the single-parameter RKD. Second, it maintains analytical tractability, enabling closed-form or semi-closed-form expressions for key statistical properties. Third, as a two-parameter model, the PRKD strikes a favourable balance between parsimony and flexibility, avoiding the excessive parametric burden that can afflict higher-dimensional generalisations of the RKD such as the alpha power reduced Kies distribution by [10], which involves an additional transformation parameter. Fourth, the power parameter directly regulates the spread and skewness of the distribution without substantially increasing model complexity. Finally, the model demonstrates strong empirical performance across diverse datasets, indicating its practical relevance in environmental, insurance, and health-related applications.

The remainder of this paper is organised as follows. In Section 2, the new bounded distribution is introduced. Some statistical properties are investigated including linear representation, reliability characteristics, quantile function, moments, moment generating function, mode, and order statistics in Section 3. In Section 4, two methods of estimation of parameters are discussed and their performance is assessed via a Monte Carlo simulation study in Section 5. The practical usefulness of the proposed distribution is demonstrated in Section 6. Finally, some conclusions are summarised and areas for further study are suggested in Section 7.

2 Model Formulation

The one-parameter Reduced Kies distribution with shape parameter $\gamma > 0$ is defined by its cumulative distribution function (CDF) and probability density function (PDF) respectively given in Equations (1) and (2).

$$G(t;\gamma) = 1 - \exp\left(-\left(\frac{t}{1-t}\right)^{\gamma}\right), \qquad t \in (0,1), \tag{1}$$

$$g(t;\gamma) = \gamma \frac{t^{\gamma-1}}{(1-t)^{\gamma+1}} \exp\left(-\left(\frac{t}{1-t}\right)^{\gamma}\right). \tag{2}$$

Using the power transformation

$$X = T^{1/\lambda}, \qquad T \sim RKD,$$

a new model called the Power Reduced Kies Distribution (PRKD) is obtained. Consequently, the CDF and PDF of the PRKD are given by Equations (3) and (4), respectively, where γ and λ are shape parameters.

$$F(x;\gamma,\lambda) = 1 - \exp\left[-\left(\frac{x^{\lambda}}{1-x^{\lambda}}\right)^{\gamma}\right], \qquad 0 < x < 1, \quad \gamma > 0, \lambda > 0, \tag{3}$$

$$f(x;\gamma,\lambda) = \frac{\gamma\lambda x^{\lambda\gamma-1}}{\left(1-x^{\lambda}\right)^{\gamma+1}} \exp\left[-\left(\frac{x^{\lambda}}{1-x^{\lambda}}\right)^{\gamma}\right] \tag{4}$$

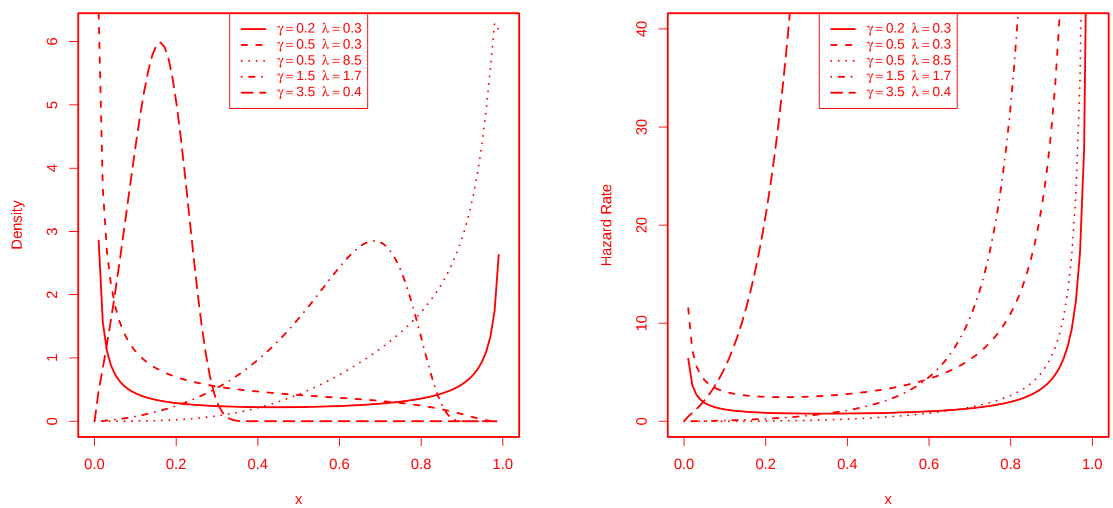

a **b**

Figure 1: (**a**) The density plots indicate that the proposed PRKD is highly flexible and capable of accommodating approximately symmetric, left-skewed, J-shaped, and reversed J-shaped density forms. (**b**) The HRF plots for selected parameter values suggest that the proposed model is capable of modelling increasing and bathtub-shaped hazard behaviours.

The density plots of the PRKD for selected parameter values are presented in Fig. 1.

3 Statistical Properties

This section investigates some mathematical/statistical properties of the proposed distribution.

3.1 Linear Representation

This section investigates some mathematical/statistical properties of the proposed distribution.

3.2 Linear Representation

Using the exponential series expansion

$$e^{-y} = \sum_{j=0}^{\infty} \frac{(-1)^j}{j!} y^j,$$

and the generalised binomial expansion

$$(1-z)^{-a} = \sum_{m=0}^{\infty} \binom{a+m-1}{m} z^m, \qquad |z| < 1, \qquad a > 0,$$

the linear representations of the CDF and PDF of the PRKD can be derived. From the CDF of the PRKD given in Equation (3), expanding the exponential term yields

$$F(x) = \sum_{j=1}^{\infty} \frac{(-1)^{j+1}}{j!} \left(\frac{x^\lambda}{1-x^\lambda} \right)^{j\gamma},$$

thus,

$$F(x) = \sum_{j=1}^{\infty} \frac{(-1)^{j+1}}{j!} x^{\lambda j\gamma} (1-x^\lambda)^{-j\gamma}.$$

Applying the generalised binomial expansion to $(1-x^\lambda)^{-j\gamma}$, (which is valid for any real $j\gamma > 0$ provided that $|x^\lambda| < 1$), yields

$$(1-x^\lambda)^{-j\gamma} = \sum_{m=0}^{\infty} \binom{j\gamma+m-1}{m} x^{\lambda m}.$$

Hence, the CDF admits the linear representation

$$F(x) = \sum_{j=1}^{\infty} \sum_{m=0}^{\infty} \frac{(-1)^{j+1}}{j!} \binom{j\gamma+m-1}{m} x^{\lambda(j\gamma+m)}. \tag{5}$$

Similarly, from the PDF of the PRKD given in Equation (4), expanding the exponential function gives

$$f(x) = \gamma\lambda x^{\lambda\gamma-1}(1-x^\lambda)^{-(\gamma+1)} \sum_{j=0}^{\infty} \frac{(-1)^j}{j!} \left(\frac{x^\lambda}{1-x^\lambda} \right)^{j\gamma},$$

$$f(x) = \gamma\lambda \sum_{j=0}^{\infty} \frac{(-1)^j}{j!} x^{\lambda(j\gamma+\gamma)-1} (1-x^\lambda)^{-(j\gamma+\gamma+1)}.$$

Again, using the generalised binomial expansion,

$$(1-x^{\lambda})^{-(j\gamma+\gamma+1)} = \sum_{m=0}^{\infty} \binom{j\gamma+\gamma+m}{m} x^{\lambda m}.$$

$$f(x) = \gamma\lambda \sum_{j=0}^{\infty}\sum_{m=0}^{\infty} \frac{(-1)^j}{j!} \binom{j\gamma+\gamma+m}{m} x^{\lambda(j\gamma+\gamma+m)-1}. \tag{6}$$

The series representations of the PRKD given in Equations (5) and (6) are valid for $0 < x < 1$, since $|x^{\lambda}| < 1$ for all $\lambda > 0$, ensuring convergence of the generalised binomial expansion.

3.3 Reliability Characteristics

Reliability measures are important tools for describing the failure behaviour and ageing properties of probability distributions. Several reliability characteristics of the PRKD are presented here.

3.3.1 Survival Function

The survival function (SF), which represents the probability that a random variable exceeds a specified value x, is defined by $S(x) = 1 - F(x)$. The SF of the PRKD is given by

$$S(x) = \exp\left[-\left(\frac{x^{\lambda}}{1-x^{\lambda}}\right)^{\gamma}\right]. \tag{7}$$

3.3.2 Hazard Rate Function

The hazard rate function (HRF), which measures the instantaneous failure rate at time x, is given by $h(x) = \frac{f(x)}{S(x)}$. Thus, the HRF of the PRKD is

$$h(x) = \frac{\gamma\lambda x^{\lambda\gamma-1}}{(1-x^{\lambda})^{\gamma+1}}. \tag{8}$$

The HRF plots for selected parameter values are displayed in Fig. 1. The plots indicate that the PRKD is capable of modelling increasing and bathtub-shaped hazard behaviours.

3.3.3 Cumulative Hazard Function

The cumulative hazard function (CHF), which measures the accumulated risk up to time x, is defined as $H(x) = -\ln[S(x)]$. Hence, for the PRKD, it is given as

$$H(x) = \left(\frac{x^{\lambda}}{1-x^{\lambda}}\right)^{\gamma}. \tag{9}$$

3.3.4 Reversed Hazard Function

The reversed hazard function (RHF), which characterises the conditional failure rate from the left tail, is defined by $r(x) = \frac{f(x)}{F(x)}$. Therefore, the RHF of the PRKD becomes

$$r(x) = \frac{\gamma\lambda x^{\lambda\gamma-1}}{(1-x^{\lambda})^{\gamma+1}\left[\exp\left\{\left(\frac{x^{\lambda}}{1-x^{\lambda}}\right)^{\gamma}\right\}-1\right]}. \tag{10}$$

3.3.5 Mill's Ratio

Mill's ratio, which describes the ratio of the survival function to the density function, is defined as $M(x) = \frac{S(x)}{f(x)}$. For the PRKD, it is obtained as

$$M(x) = \frac{(1-x^{\lambda})^{\gamma+1}}{\gamma\lambda x^{\lambda\gamma-1}}. \tag{11}$$

3.3.6 Elasticity Function

The elasticity function measures the relative rate of change of the hazard function and is defined by $E(x) = \frac{xh'(x)}{h(x)}$, where $h'(x)$ is the first derivative of the HRF. For the PRKD, the elasticity function is obtained as

$$E(x) = \lambda\gamma - 1 + \frac{\lambda(\gamma+1)x^{\lambda}}{1-x^{\lambda}}. \tag{12}$$

3.4 Quantile Function

The quantile function (QF) is obtained by inverting the CDF of a distribution. It is particularly useful in random variate generation, simulation studies, and the computation of descriptive measures. From the CDF of the PRKD, the QF is obtained by solving $F(x) = u$ for x. Thus,

$$Q(u) = \left[1 + \{-\ln(1-u)\}^{-1/\gamma}\right]^{-1/\lambda}, \quad 0 < u < 1. \tag{13}$$

The QF may be used to generate random observations from the PRKD through the inverse transformation method. Setting $u = 0.5$ in Equation (13), the median of the PRKD is obtained as

$$Median = \left[1 + (\ln 2)^{-1/\gamma}\right]^{-1/\lambda}. \tag{14}$$

3.5 Mode

The mode of a distribution is the value of x at which the PDF attains its maximum value. For the PRKD, the mode is obtained by solving

$$\frac{d}{dx}\ln[f(x)] = 0.$$

Using the PDF of the PRKD given in Equation (4), the log-density function becomes

$$\ln f(x) = \ln(\gamma\lambda) + (\lambda\gamma - 1)\ln x - (\gamma + 1)\ln\left(1 - x^{\lambda}\right) - \left(\frac{x^{\lambda}}{1 - x^{\lambda}}\right)^{\gamma},$$

differentiating with respect to x yields

$$\frac{d}{dx}\ln f(x) = \frac{\lambda\gamma - 1}{x} + \frac{\lambda(\gamma + 1)x^{\lambda - 1}}{1 - x^{\lambda}} - \frac{d}{dx}\left(\frac{x^{\lambda}}{1 - x^{\lambda}}\right)^{\gamma},$$

but

$$\frac{d}{dx}\left(\frac{x^{\lambda}}{1 - x^{\lambda}}\right)^{\gamma} = \frac{\lambda\gamma x^{\gamma - 1}x^{\lambda(\gamma - 1)}}{\left(1 - x^{\lambda}\right)^{2}\left(1 - x^{\lambda}\right)^{\gamma - 1}} = \frac{\lambda\gamma x^{\lambda\gamma - 1}}{\left(1 - x^{\lambda}\right)^{\gamma + 1}},$$

thus

$$\frac{d}{dx}\ln f(x) = \frac{\lambda\gamma - 1}{x} + \frac{\lambda(\gamma + 1)x^{\lambda - 1}}{1 - x^{\lambda}} - \frac{\lambda\gamma x^{\lambda\gamma - 1}}{\left(1 - x^{\lambda}\right)^{\gamma + 1}},$$

The mode x_m satisfies

$$\frac{\lambda\gamma - 1}{x_m} + \frac{\lambda(\gamma + 1)x_m^{\lambda - 1}}{1 - x_m^{\lambda}} - \frac{\lambda\gamma x_m^{\lambda\gamma - 1}}{\left(1 - x_m^{\lambda}\right)^{\gamma + 1}} = 0,$$

$$(\lambda\gamma - 1)\left(1 - x_m^{\lambda}\right)^{\gamma + 1} + \lambda(\gamma + 1)x_m^{\lambda}\left(1 - x_m^{\lambda}\right)^{\gamma} - \lambda\gamma x_m^{\lambda\gamma} = 0, \tag{15}$$

for all $0 < x < 1$, $\gamma > 0$, and $\lambda > 0$.

Hence, Mode$(X) = x_m$, where x_m, is the unique root of the Equation (15) that maximises the density. It is clear that Equation (15) does not admit a closed-form solution. The mode must therefore be obtained numerically using root-finding algorithms such as the *uniroot()* function in ***R*** software or the Newton-Raphson method. The computed modal values for selected parameter combinations are presented in Table 1.

The numerical results in Table 1 show that the mode of the PRKD is strongly influenced by the parameter γ. As γ increases, the modal value shifts steadily towards the upper boundary of the unit interval, indicating higher concentration of probability mass around larger observations. Conversely, increasing λ produces a slight reduction in the modal values for fixed γ, suggesting that γ plays a moderating role in controlling the peak location of the distribution.

3.6 Order Statistic

Order statistics play an important role in reliability analysis, life testing, inferential procedures, and extreme value modelling. Let $X_{(1)}, X_{(2)}, \ldots, X_{(n)}$ denote the order statistics obtained from a random sample of size n drawn from the PRKD. The CDF of the r^{th} order statistic $X_{(r)}$ is defined by

$$F_{X_{(r)}}(x) = \sum_{k=r}^{n} \binom{n}{k} [F(x)]^k [1 - F(x)]^{n-k}.$$

From the CDF of the PRKD given in Equation (3), the CDF of the r^{th} order statistic becomes

$$F_{X_{(r)}}(x) = \sum_{k=r}^{n} \binom{n}{k} \left[1 - \exp\left\{-\left(\frac{x^\lambda}{1 - x^\lambda}\right)^\gamma\right\}\right]^k \exp\left[-(n-k)\left(\frac{x^\lambda}{1 - x^\lambda}\right)^\gamma\right]. \tag{16}$$

For the minimum order statistic $r = 1$, $F_{X_{(1)}}(x) = 1 - [1 - F(x)]^n$. Hence,

$$F_{X_{(1)}}(x) = 1 - \exp\left[-n\left(\frac{x^\lambda}{1 - x^\lambda}\right)^\gamma\right]. \tag{17}$$

Similarly, for the maximum order statistic $r = n$, $F_{X_{(n)}}(x) = [F(x)]^n$, which gives

$$F_{X_{(n)}}(x) = \left[1 - \exp\left\{-\left(\frac{x^\lambda}{1 - x^\lambda}\right)^\gamma\right\}\right]^n. \tag{18}$$

The PDF of the r^{th} order statistic is given by

$$f_{X_{(r)}}(x) = \frac{n!}{(r-1)!(n-r)!} [F(x)]^{r-1} [1 - F(x)]^{n-r} f(x),$$

Table 1: Numerical values of the mode of the PRKD for selected parameter combinations.

γ	λ	Mode	γ	λ	Mode	γ	λ	Mode
1.5	1.1	0.6672	1.5	3.2	0.6334	1.5	4.6	0.6316
2.2	1.1	0.7715	2.2	3.2	0.7341	2.2	4.6	0.7319
2.8	1.1	0.8197	2.8	3.2	0.7850	2.8	4.6	0.7828
3.5	1.1	0.8552	3.5	3.2	0.8243	3.5	4.6	0.8223
4.5	1.1	0.8870	4.5	3.2	0.8607	4.5	4.6	0.8589
5.3	1.1	0.9039	5.3	3.2	0.8806	5.3	4.6	0.8790
1.5	2.5	0.6357	1.5	3.8	0.6324	1.5	5.9	0.6310
2.2	2.5	0.7370	2.2	3.8	0.7328	2.2	5.9	0.7310
2.8	2.5	0.7877	2.8	3.8	0.7837	2.8	5.9	0.7820
3.5	2.5	0.8268	3.5	3.8	0.8232	3.5	5.9	0.8215
4.5	2.5	0.8629	4.5	3.8	0.8597	4.5	5.9	0.8583
5.3	2.5	0.8825	5.3	3.8	0.8797	5.3	5.9	0.8783

substituting the CDF and PDF of the PRKD in Equation (3) and (4) yields the PDF of the r^{th} order statistic as

$$f_{X_{(r)}}(x) = \frac{n!}{(r-1)!(n-r)!} \frac{\gamma\lambda x^{\lambda\gamma-1}}{(1-x^{\lambda})^{\gamma+1}} \left[1 - \exp\left\{-\left(\frac{x^{\lambda}}{1-x^{\lambda}}\right)^{\gamma}\right\}\right]^{r-1} \exp\left[-(n-r+1)\left(\frac{x^{\lambda}}{1-x^{\lambda}}\right)^{\gamma}\right]. \tag{19}$$

For the smallest order statistic $r = 1$, $f_{X_{(1)}}(x) = n[1 - F(x)]^{n-1} f(x)$. Therefore,

$$f_{X_{(1)}}(x) = \frac{n\gamma\lambda x^{\lambda\gamma-1}}{(1-x^{\lambda})^{\gamma+1}} \exp\left[-n\left(\frac{x^{\lambda}}{1-x^{\lambda}}\right)^{\gamma}\right]. \tag{20}$$

Similarly, for the largest order statistic $r = n$, $f_{X_{(n)}}(x) = n[F(x)]^{n-1} f(x)$, which gives

$$f_{X_{(n)}}(x) = \frac{n\gamma\lambda x^{\lambda\gamma-1}}{(1-x^{\lambda})^{\gamma+1}} \left[1 - \exp\left\{-\left(\frac{x^{\lambda}}{1-x^{\lambda}}\right)^{\gamma}\right\}\right]^{n-1} \exp\left[-\left(\frac{x^{\lambda}}{1-x^{\lambda}}\right)^{\gamma}\right]. \tag{21}$$

3.7 Moments

Moments are fundamental measures used to describe important characteristics of a probability distribution such as central tendency, variability, skewness, and kurtosis. Let $X \sim PRKD(\gamma, \lambda)$. The r^{th} ordinary moment of X is defined by

$$\mu_r' = E(X^r) = \int_0^1 x^r f(x) dx$$

From the PDF of the PRKD in Equation (4), the r^{th} moment becomes

$$\mu_r' = \gamma\lambda \int_0^1 \frac{x^{r+\lambda\gamma-1}}{(1-x^{\lambda})^{\gamma+1}} \exp\left[-\left(\frac{x^{\lambda}}{1-x^{\lambda}}\right)^{\gamma}\right] dx.$$

Let $y = \left(\frac{x^{\lambda}}{1-x^{\lambda}}\right)^{\gamma}$, then, $x = \left(\frac{y^{1/\gamma}}{1+y^{1/\gamma}}\right)^{1/\lambda}$, and after simplification, the integral reduces to

$$\mu_r' = \int_0^{\infty} \left(\frac{y^{1/\gamma}}{1+y^{1/\gamma}}\right)^{r/\lambda} e^{-y} dy.$$

Using the binomial expansion

$$(1+z)^{-a} = \sum_{j=0}^{\infty} (-1)^j \binom{a+j-1}{j} z^j, \qquad |z| < 1,$$

the r^{th} moment can be expressed as

$$\mu_r' = \sum_{j=0}^{\infty} (-1)^j \binom{\frac{r}{\lambda}+j-1}{j} \Gamma\left(\frac{r}{\lambda\gamma} + j + 1\right). \tag{22}$$

Equivalently, using the Gamma function representation of the binomial coefficient,

$$\mu_r' = \sum_{j=0}^{\infty} \frac{(-1)^j \Gamma\left(\frac{r}{\lambda} + j\right)}{j! \Gamma\left(\frac{r}{\lambda}\right)} \Gamma\left(\frac{r}{\lambda\gamma} + j + 1\right). \tag{23}$$

The expressions in Equations (22) and (23) provide the ordinary moments of the PRKD and facilitate the computation of important descriptive measures such as the mean, variance, skewness, and kurtosis. Numerical evaluation of Equation (23) was carried out using R software, and the resulting measures for selected parameter combinations are presented in Table 2.

Table 2: Mean, variance, skewness and kurtosis coefficients for different parameter values of PRKD.

γ	λ	Mean	Variance	Skewness	Kurtosis	γ	λ	Mean	Variance	Skewness	Kurtosis
0.6	0.7	0.3000	0.0752	0.6022	2.0730	0.6	2.5	0.6107	0.0657	-0.4933	2.1435
1.2	0.7	0.3029	0.0343	0.2284	2.1106	1.2	2.5	0.6755	0.0253	-0.9283	3.5005
1.8	0.7	0.3136	0.0199	-0.0727	2.2795	1.8	2.5	0.7025	0.0126	-1.1393	4.5185
2.4	0.7	0.3228	0.0131	-0.2856	2.5455	2.4	2.5	0.7167	0.0073	-1.2442	5.1858
3.6	0.7	0.3353	0.0068	-0.5524	3.0955	3.6	2.5	0.7310	0.0033	-1.3194	5.8490
0.6	1.2	0.4285	0.0828	0.1085	1.7150	0.6	3.5	0.6869	0.0515	-0.7472	2.6355
1.2	1.2	0.4691	0.0380	-0.3123	2.2579	1.2	3.5	0.7506	0.0179	-1.1670	4.3297
1.8	1.2	0.4929	0.0212	-0.5807	2.8658	1.8	3.5	0.7748	0.0085	-1.3439	5.4275
2.4	1.2	0.5076	0.0133	-0.7511	3.4012	2.4	3.5	0.7870	0.0048	-1.4165	6.0561
3.6	1.2	0.5242	0.0065	-0.9385	4.1685	3.6	3.5	0.7989	0.0021	-1.4434	6.5498

The results in Table 2 indicate that the mean of the PRKD increases with both γ and λ, while the variance decreases steadily, reflecting increasing concentration of observations around the centre of the distribution. Furthermore, the skewness coefficient changes from positive to negative as the parameter values increase, showing that the PRKD is capable of modelling both right-skewed and left-skewed data. The kurtosis values also increase with larger parameter values, indicating greater peakedness and heavier tail behaviour, thereby demonstrating the substantial flexibility of the PRKD in modelling diverse unit interval data.

3.8 Moments Generating Function

The moment generating function (MGF) of a random variable $X \sim PRKD(\gamma, \lambda)$ is defined by $M_X(t) = E\left(e^{tX}\right)$, provided the expectation exists in a neighbourhood of $t = 0$. Using the Maclaurin series expansion of the exponential function,

$$e^{tX} = \sum_{m=0}^{\infty} \frac{t^m X^m}{m!},$$

the MGF can be expressed in terms of the ordinary moments as

$$M_X(t) = \sum_{m=0}^{\infty} \frac{t^m}{m!} E(X^m) = \sum_{m=0}^{\infty} \frac{t^m}{m!} \mu_m',$$

where $\mu'_m = E(X^m)$ denotes the m^{th} raw moment. Substituting the general moment expression of the PRKD yields

$$M_X(t) = \sum_{m=0}^{\infty} \frac{t^m}{m!} \sum_{j=0}^{\infty} \frac{(-1)^j}{j!} \binom{\frac{m}{\lambda} + j - 1}{j} \Gamma\left(\frac{m}{\lambda\gamma} + j + 1\right).$$

Equivalently, in Gamma-function form,

$$M_X(t) = \sum_{m=0}^{\infty} \frac{t^m}{m!} \sum_{j=0}^{\infty} \frac{(-1)^j}{j!} \frac{\Gamma\left(\frac{m}{\lambda} + j\right)}{\Gamma\left(\frac{m}{\lambda}\right)} \Gamma\left(\frac{m}{\lambda\gamma} + j + 1\right). \tag{24}$$

Equation (24) expresses the MGF of the PRKD as a double infinite series. Its convergence is ensured for values of t in a neighbourhood of zero, provided that the corresponding moments exist.

4 Estimation Methods

This section presents parameter estimation procedures for the PRKD, focusing on the Maximum Likelihood Estimation (MLE) and the Maximum Product of Spacings Estimation (MPSE) methods.

4.1 Maximum Likelihood Estimation

Let $x_1, x_2, ..., x_n$ be an independent and identically distributed sample from the PRKD with parameters (γ, λ). The likelihood function is

$$L(\gamma, \lambda) = \prod_{i=1}^{n} f(x_i; \gamma, \lambda),$$

and the corresponding log-likelihood function is

$$\ell(\gamma, \lambda) = \sum_{i=1}^{n} \ln f(x_i; \gamma, \lambda).$$

Substituting the PRKD density in Equation (4), the log-likelihood function becomes

$$\ell(\gamma, \lambda) = n \ln(\gamma\lambda) + (\lambda\gamma - 1) \sum_{i=1}^{n} \ln x_i - (\gamma + 1) \sum_{i=1}^{n} \ln\left(1 - {x_i}^{\lambda}\right) - \sum_{i=1}^{n} \left(\frac{{x_i}^{\lambda}}{1 - {x_i}^{\lambda}}\right)^{\gamma}. \tag{25}$$

The score functions are obtained by differentiating Equation (25) with respect to γ and λ, which yield

$$\frac{\partial \ell}{\partial \gamma} = \frac{n}{\gamma} + \lambda \sum_{i=1}^{n} \ln x_i - \sum_{i=1}^{n} \ln\left(1 - {x_i}^{\lambda}\right) - \sum_{i=1}^{n} \left(\frac{{x_i}^{\lambda}}{1 - {x_i}^{\lambda}}\right)^{\gamma} \ln\left(\frac{{x_i}^{\lambda}}{1 - {x_i}^{\lambda}}\right),$$

$$\frac{\partial \ell}{\partial \lambda} = \frac{n}{\lambda} + \gamma \sum_{i=1}^{n} \ln x_i + (\gamma + 1) \sum_{i=1}^{n} \frac{x_i^{\lambda} \ln x_i}{1 - x_i^{\lambda}} - \gamma \sum_{i=1}^{n} \left(\frac{x_i^{\lambda}}{1 - x_i^{\lambda}}\right)^{\gamma} \frac{x_i^{\lambda} \ln x_i}{1 - x_i^{\lambda}}.$$

The maximum likelihood estimators $\widehat{\gamma}_{MLE}$ and $\widehat{\lambda}_{MLE}$ are obtained by solving the nonlinear system

$$\frac{\partial \ell}{\partial \gamma} = 0, \quad \frac{\partial \ell}{\partial \lambda} = 0.$$

Since closed-form solutions are not available, numerical optimisation techniques are required.

4.2 Maximum Product of Spacings Estimation

Let $x_{(1)}, x_{(2)}, ..., x_{(r)}$ denote the ordered sample observations from the PRKD. The MPSE method is based on maximising the geometric mean of spacings defined from the CDF. The spacing function is defined as

$$D_r(\gamma, \lambda) = F(x_{(r)}; \gamma, \lambda) - F(x_{(r-1)}; \gamma, \lambda), \quad r = 1, 2, \dots, m+1,$$

with boundary conditions $F(x_{(0)}) = 0, \quad F(x_{(m+1)}) = 1$. The objective function for MPS estimation is then

$$M(\gamma, \lambda) = \frac{1}{m+1} \sum_{r=1}^{m+1} \ln D_r(\gamma, \lambda).$$

For the PRKD, using the CDF in Equation (3), the spacings simplify to

$$D_r(\gamma, \lambda) = \exp\left[-\left(\frac{x_{(r-1)}^{\lambda}}{1 - x_{(r-1)}^{\lambda}} \right)^{\gamma} \right] - \exp\left[-\left(\frac{x_{(r)}^{\lambda}}{1 - x_{(r)}^{\lambda}} \right)^{\gamma} \right]. \tag{26}$$

The MPS estimators $\widehat{\gamma}_{MPSE}$ and $\widehat{\lambda}_{MPSE}$ are obtained by maximising Equation (26) with respect to γ and λ. This optimisation is typically carried out using numerical routines due to the absence of closed-form solutions.

5 Simulation

A Monte Carlo simulation study was conducted to evaluate the performance of the MLE and MPSE for the PRKD via the use of the mean estimates and mean squared error (MSE). The simulations were implemented in ***R*** software using the *optim()* function with the *L-BFGS-B* optimisation algorithm under multiple parameter configurations and sample sizes. For each setting, $R = 1,000$ replications were considered to ensure numerical stability and accuracy of the results.

The results of the simulation are presented in Table 3. Based on the results of the simulation, the following observations can be suggested:

1. For both MLE and MPSE, the estimates of and improve steadily as the sample size increases, demonstrating consistency of both estimators.
2. As sample size approaches $n = 1000$, both estimators converge closely to the true parameter values, although MPSE maintains marginally lower dispersion in most cases.
3. The MSE decreases monotonically with increasing sample size across all parameter settings, confirming the asymptotic efficiency of both methods.

Table 3: Simulation results of the PRKD.

n	(γ, λ)	MLE				MPSE			
		Mean($\hat{\gamma}$)	Mean($\hat{\lambda}$)	MSE($\hat{\gamma}$)	MSE($\hat{\lambda}$)	Mean($\hat{\gamma}$)	Mean($\hat{\lambda}$)	MSE($\hat{\gamma}$)	MSE($\hat{\lambda}$)
25	(0.75, 0.45)	0.8352	0.5068	0.0218	0.0076	0.7598	0.5262	0.0113	0.0106
50	(0.75, 0.45)	0.7967	0.4906	0.0092	0.0035	0.7532	0.5002	0.0062	0.0044
100	(0.75, 0.45)	0.7761	0.4787	0.0037	0.0017	0.7530	0.4848	0.0027	0.0022
250	(0.75, 0.45)	0.7668	0.4674	0.0015	0.0007	0.7549	0.4699	0.0011	0.0008
500	(0.75, 0.45)	0.7601	0.4626	0.0007	0.0003	0.7528	0.4638	0.0006	0.0003
1000	(0.75, 0.45)	0.7569	0.4591	0.0003	0.0002	0.7534	0.4596	0.0003	0.0002
25	(1.35, 1.15)	1.4277	1.1484	0.0575	0.0154	1.2652	1.1567	0.0479	0.0154
50	(1.35, 1.15)	1.3910	1.1508	0.0250	0.0073	1.2940	1.1555	0.0234	0.0074
100	(1.35, 1.15)	1.3646	1.1497	0.0109	0.0037	1.3076	1.1522	0.0116	0.0037
250	(1.35, 1.15)	1.3577	1.1498	0.0046	0.0015	1.3298	1.1509	0.0047	0.0015
500	(1.35, 1.15)	1.3540	1.1489	0.0020	0.0007	1.3381	1.1494	0.0021	0.0007
1000	(1.35, 1.15)	1.3523	1.1499	0.0010	0.0004	1.3433	1.1502	0.0011	0.0004
25	(1.45, 1.95)	1.5330	1.9466	0.0664	0.0387	1.3589	1.9613	0.0553	0.0393
50	(1.45, 1.95)	1.4939	1.9508	0.0289	0.0183	1.3898	1.9586	0.0271	0.0186
100	(1.45, 1.95)	1.4656	1.9494	0.0126	0.0093	1.4044	1.9534	0.0134	0.0093
250	(1.45, 1.95)	1.4582	1.9497	0.0053	0.0037	1.4282	1.9513	0.0055	0.0037
500	(1.45, 1.95)	1.4543	1.9482	0.0023	0.0017	1.4372	1.9491	0.0024	0.0017
1000	(1.45, 1.95)	1.4524	1.9498	0.0012	0.0009	1.4428	1.9502	0.0012	0.0009
25	(2.05, 3.25)	2.1653	3.2413	0.1345	0.0560	1.9211	3.2613	0.1125	0.0565
50	(2.05, 3.25)	2.1113	3.2488	0.0585	0.0264	1.9652	3.2595	0.0548	0.0267
100	(2.05, 3.25)	2.0716	3.2483	0.0257	0.0134	1.9857	3.2538	0.0273	0.0134
250	(2.05, 3.25)	2.0613	3.2491	0.0107	0.0053	2.0193	3.2515	0.0111	0.0054
500	(2.05, 3.25)	2.0558	3.2477	0.0047	0.0025	2.0317	3.2488	0.0049	0.0025
1000	(2.05, 3.25)	2.0534	3.2497	0.0025	0.0013	2.0398	3.2502	0.0025	0.0013

4. MPSE generally yields smaller MSE values than MLE, particularly for small and moderate sample sizes, indicating superior finite-sample performance.
5. MLE exhibits slightly higher bias in small samples, especially for larger values of λ, while MPSE shows greater stability in early sample regimes.

6 Applications

This section demonstrates the applicability and flexibility of the proposed PRKD in modelling real data arising from diverse fields. The performance of the PRKD is assessed against a set of competing unit distributions using standard model selection and goodness-of-fit diagnostics. All the computations were performed using the *adequacymodel* package in ***R*** software [25]. The proposed PRKD is compared with twelve competing unit models consisting of the baseline distribution, some of its generalisations, and other well-known unit distributions namely: Marshall-Olkin Reduced Kies (MORKD) by [2], Exponentiated Reduced Kies (ERKD) by [22], Reduced Kies (RKD) by [21], Topp-Leone (TLD) by [32], Alpha Power Topp-Leone (APTLD) by [8], Beta (BD) by [7], Kumaraswamy (KD) by [23], Unit-Gompertz (UGD) by [27], Unit Muth (UMD) by [26], Unit Weibull (UWD) by [28], Unit Burr III (UBIIID) by [29], and Unit Burr XII (UBXIID) by [19]. The PDFs of these competing models, defined for all $\gamma > 0, \lambda > 0,$ and $0 < x < 1$, are presented in Table 4 for completeness and ease of reference.

Table 4: List of fitted models.

Model	PDF
PRKD	$f(x;\gamma,\lambda) = \gamma\lambda \frac{x^{\lambda\gamma-1}}{(1-x^{\lambda})^{\gamma+1}} \exp\left(-\left(\frac{x^{\lambda}}{1-x^{\lambda}}\right)^{\gamma}\right)$
MORKD	$f(x;\gamma,\lambda) = \frac{\gamma\lambda x^{\gamma-1}(1-x)^{-\gamma-1}\exp\left(-\left(\frac{x}{1-x}\right)^{\gamma}\right)}{\left(1-(1-\lambda)\exp\left(-\left(\frac{x}{1-x}\right)^{\gamma}\right)\right)^{2}}$
ERKD	$f(x;\gamma,\lambda) = \gamma\lambda \frac{x^{\gamma-1}}{(1-x)^{\gamma+1}} \exp\left(-\left(\frac{x}{1-x}\right)^{\gamma}\right)\left(1-\exp\left(-\left(\frac{x}{1-x}\right)^{\gamma}\right)\right)^{\lambda-1}$
RKD	$f(x;\gamma) = \gamma x^{\gamma-1}(1-x)^{-\gamma-1}\exp\left(-\left(\frac{x}{1-x}\right)^{\gamma}\right)$
TLD	$f(x;\gamma) = 2\gamma(1-x)\left(1-(1-x)^{2}\right)^{\gamma-1}$
APTLD	$f(x;\gamma,\lambda) = 2\gamma(1-x)\left(1-(1-x)^{2}\right)^{\gamma-1}\frac{\ln(\lambda)}{\lambda-1}\lambda^{\left(1-(1-x)^{2}\right)^{\gamma}}$
BD	$f(x;\gamma,\lambda) = \frac{\Gamma(\gamma+\lambda)}{\Gamma(\gamma)\Gamma(\lambda)}x^{\gamma-1}(1-x)^{\lambda-1}$
KD	$f(x;\gamma,\lambda) = \gamma\lambda x^{\gamma-1}(1-x^{\gamma})^{\lambda-1}$
UGD	$f(x;\gamma,\lambda) = \gamma\lambda x^{-\lambda-1}\exp\left(\gamma\left(1-x^{-\lambda}\right)\right)$
UMD	$f(x;\gamma,\lambda) = \frac{1}{\lambda}x^{-\left(\frac{\gamma}{\lambda}+1\right)}\exp\left(\frac{1}{\gamma}\left(1-x^{-\frac{\gamma}{\lambda}}\right)\right)$
UWD	$f(x;\gamma,\lambda) = \frac{1}{x}\gamma\lambda(-\ln x)^{\lambda-1}\exp\left(-\gamma(-\ln x)^{\lambda}\right)$
UBIIID	$f(x;\gamma,\lambda) = \gamma\lambda x^{-2}\left(1+\left(\frac{1}{x}-1\right)^{\lambda}\right)^{-\gamma-1}\left(\frac{1}{x}-1\right)^{\lambda-1}$
UBXIID	$f(x;\gamma,\lambda) = \gamma\lambda x^{-1}(-\ln x)^{\lambda-1}\left(1+(-\ln x)^{\lambda}\right)^{-\gamma-1}$

6.1 Model Selection Criteria

The parameters of all competing models are estimated via the MLE approach. The goodness-of-fit of each model is evaluated using the following criteria:

- Akaike Information Criterion (AIC): $AIC = -2\ell + 2k$,
- Bayesian Information Criterion (BIC): $BIC = -2\ell + k\ln n$,

- Corrected Akaike Information Criterion (CAIC): $CAIC = -2\ell + \frac{2kn}{n-k-1}$,
- Hannan-Quinn Information Criterion (HQIC): $HQIC = -2\ell + 2k\ln(\ln n)$,
- Kolmogorov-Smirnov (KS) test statistic: $KS = \sup_x |F_n(x) - F(x)|$,
- associated p-value of the KS test (KSpv),

where ℓ = maximised log-likelihood function, k = numbers of parameters and n = sample size, $F_n(x)$ is the empirical distribution function and $F(x)$ is the theoretical CDF of the fitted model.

6.2 Data Source and Description

A total of four real datasets from different scientific and applied domains are considered to evaluate the applicability and flexibility of the proposed PRKD. The first two datasets relate to environmental and soil science measurements, while the remaining two datasets arise from biomedical and actuarial applications.

The first dataset consists of observations on Permanent Wilting Point (PWP), which represents the minimum soil moisture level at which plants are unable to extract water from the soil.

The second dataset comprises soil moisture content measurements. Both datasets were reported by [24] and were subsequently analysed by [5], thereby providing useful benchmark datasets for comparative modelling studies.

The third dataset contains recovery rates associated with COVID-19 infections in Spain from 3 March 2020 to 7 May 2020 and consists of 66 observations. This dataset was previously analysed by [2].

The fourth dataset represents monthly unemployment insurance metrics recorded from July 2008 to April 2013 and contains 58 observations. The data were reported by the Maryland Department of Labor, USA. This dataset was subsequently analysed by [33] and [10]. The dataset is publicly available at https://catalog.data.gov/dataset/unemployment-insurance-data-july-2008-to-april-2013.

The observations corresponding to the four datasets are presented in Table 5. In addition, the descriptive statistics associated with these datasets are reported in Table 6, and are supported by the box plots in Fig. 2.

Table 5: Observations of the datasets.

Dataset	Observations
Permanent Wilting Points	0.0179, 0.0798, 0.0959, 0.0444, 0.0938, 0.0443, 0.0917, 0.0882, 0.0439, 0.049, 0.0774, 0.0171, 0.0305, 0.0757, 0.0468.
Soil Moisture Content	0.0821, 0.0561, 0.0202, 0.051, 0.0041, 0.0226, 0.0556, 0.0829, 0.0062, 0.0695, 0.0557, 0.0243, 0.0083, 0.0532, 0.0118.
Recovery Rates	0.6670, 0.5000, 0.5000, 0.4286, 0.7500, 0.6531, 0.5161, 0.7895, 0.7689, 0.6873, 0.5200, 0.7251, 0.6375, 0.6078, 0.6289, 0.5712, 0.5923, 0.6061, 0.5924, 0.5921, 0.5592, 0.5954, 0.6164, 0.6455, 0.6725, 0.6838, 0.6850, 0.6947, 0.7210, 0.7315, 0.7412, 0.7508, 0.7519, 0.7547, 0.7645, 0.7715, 0.7759, 0.7807, 0.7838, 0.7847, 0.7871, 0.7902, 0.7934, 0.7913, 0.7962, 0.7971, 0.7977, 0.8007, 0.8038, 0.8289, 0.8322, 0.8354, 0.8371, 0.8387, 0.8456, 0.8490, 0.8535, 0.8547, 0.8564, 0.8580, 0.8604, 0.8628, 0.6586, 0.7070, 0.7963, 0.8516.
Insurance	0.188, 0.202, 0.195, 0.385, 0.489, 0.545, 0.541, 0.535, 0.521, 0.508, 0.512, 0.507, 0.519, 0.493, 0.487, 0.460, 0.490, 0.460, 0.490, 0.500, 0.400, 0.350, 0.370, 0.410, 0.400, 0.400, 0.410, 0.400, 0.420, 0.450, 0.450, 0.420, 0.390, 0.340, 0.360, 0.400, 0.440, 0.390, 0.410, 0.450, 0.460, 0.470, 0.490, 0.460, 0.410, 0.390, 0.400, 0.440, 0.420, 0.420, 0.450, 0.470, 0.530, 0.420, 0.490, 0.440, 0.420, 0.400.

Table 6: Descriptive analysis of the considered datasets.

Dataset	n	Mean	Median	Mode	Min	Max	SD	Skewness	Kurtosis
PWP	15	0.0598	0.0490	0.0179	0.0171	0.0959	0.0276	-0.1083	1.6247
Soil Moisture	15	0.0402	0.0510	0.0821	0.0041	0.0829	0.0276	0.1083	1.6247
Recovery Rates	66	0.7240	0.7533	0.5000	0.4286	0.8628	0.1086	-0.7049	2.6021
Insurance	58	0.4322	0.4400	0.4000	0.1880	0.5450	0.0754	-1.3764	5.8260

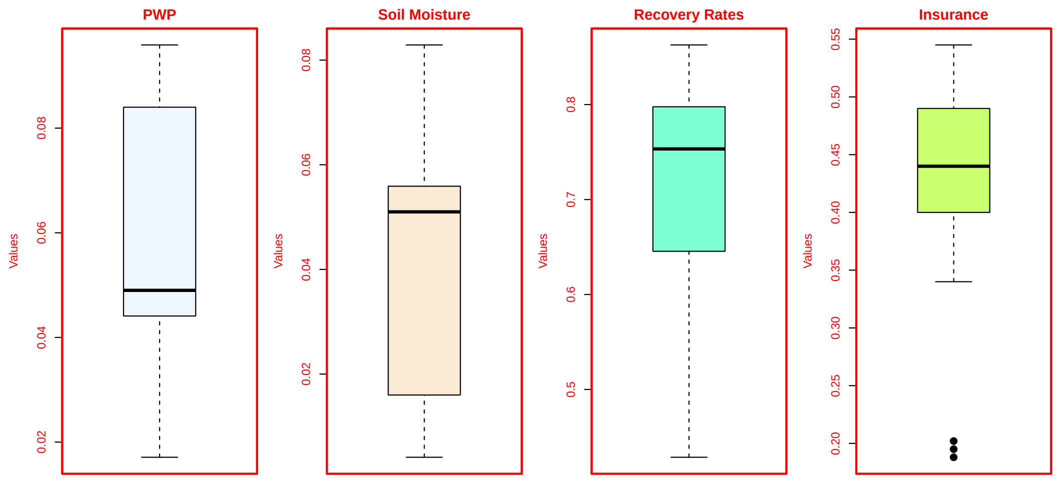

a

Figure 2: Box plots of the datasets.

Table 6 and Fig. 1 jointly reveal noticeable differences in the distributional characteristics of the four datasets in terms of location, dispersion, skewness, and tail behaviour. The PWP and Soil Moisture Content datasets exhibit relatively low variability with mild opposite skewness patterns, whereas the Recovery Rates and Insurance datasets display stronger negative skewness with observations concentrated towards the upper region of the unit interval. Furthermore, the high kurtosis observed in the Insurance dataset, together with the asymmetry displayed in the box plots, confirms the heterogeneous nature of the datasets and highlights the flexibility required of an appropriate unit distribution model such as the PRKD.

6.3 Inferential Results and Discussion

Tables 7 - 10 present the maximum likelihood estimates, model selection criteria, and goodness-of-fit statistic for the PRKD and the competing unit distributions fitted to the four datasets under consideration. The comparative analysis is based on the maximised ℓ, AIC, BIC, CAIC, HQIC, KS statistic, and the corresponding KSpv. In general, the PRKD demonstrates competitive fitting performance across the datasets, indicating its strong flexibility and adaptability for modelling bounded continuous data.

For the Permanent Wilting Point dataset in Table 7, the PRKD provides the smallest values of AIC, BIC, CAIC, HQIC, and KS statistic together with the largest KSpv among all competing models. These results indicate that the proposed model achieves the best overall fit for the dataset. The RKD, ERKD, UBIIID, and UBXIID exhibit considerably larger KS statistics and extremely small p-values, suggesting inadequate fitting performance.

Similarly, for the Soil Moisture Content dataset reported in Table 8, the PRKD again outperforms most competing models in terms of the information criteria and goodness-of-fit measures. Although the Beta distribution yields a slightly smaller KS statistic and larger KSpv, the PRKD attains substantially

Table 7: Numerical values for analyzing the PWP dataset.

Models	γ	λ	ℓ	AIC	BIC	CAIC	HQIC	KS	KSpv
PRKD	4.9113	0.2595	-33.6449	-63.2899	-61.8738	-62.2899	-63.3050	0.1838	0.6265
MORKD	2.2003	0.0020	-30.8806	-57.7612	-56.3451	-56.7612	-57.7763	0.2174	0.4178
ERKD	4.2638	0.0810	-14.2476	-24.4951	-23.0790	-23.4951	-24.5102	0.5394	0.0001
RKD	0.4661	-	-9.4758	-16.9515	-16.2435	-16.6438	-16.9591	0.7037	0.0000
TLD	0.4377	-	-16.3448	-30.6896	-29.9816	-30.3819	-30.6972	0.5249	0.0002
APTLD	1.0036	0.0005	-26.7827	-49.5655	-48.1494	-48.5655	-49.5806	0.2759	0.1682
BD	1.8113	24.6944	-30.6630	-57.3259	-55.9098	-56.3259	-57.3410	0.2360	0.3213
KD	1.2412	25.5520	-29.4424	-54.8848	-53.4687	-53.8848	-54.8999	0.2390	0.3072
UGD	0.0046	1.6738	-29.6382	-55.2763	-53.8602	-54.2763	-55.2914	0.2284	0.3587
UMD	17.2400	17.6443	-27.0054	-50.0108	-48.5947	-49.0108	-50.0259	0.4026	0.0104
UWD	0.0023	5.3136	-30.9713	-57.9425	-56.5264	-56.9425	-57.9576	0.1941	0.5592
UBIIID	0.0773	4.4594	-14.2474	-24.4947	-23.0786	-23.4947	-24.5098	0.5385	0.0001
UBXIID	0.1384	6.8488	-12.2868	-20.5736	-19.1575	-19.5736	-20.5887	0.5542	0.0001

Table 8: Numerical values for analyzing the soil moisture content dataset.

Models	γ	λ	ℓ	AIC	BIC	CAIC	HQIC	KS	KSpv
PRKD	3.4037	0.2265	-34.7801	-65.5602	-64.1441	-64.5602	-65.5752	0.2139	0.4380
MORKD	1.6493	0.0035	-32.5470	-61.0940	-59.6779	-60.0940	-61.1091	0.2310	0.3458
ERKD	3.5964	0.0790	-20.1826	-36.3651	-34.9490	-35.3651	-36.3802	0.4949	0.0006
RKD	0.3806	-	-15.2868	-28.5736	-27.8655	-28.2659	-28.5811	0.6699	0.0000
TLD	0.3460	-	-22.2086	-42.4172	-41.7092	-42.1096	-42.4248	0.4708	0.0014
APTLD	0.7972	0.0004	-31.2877	-58.5754	-57.1593	-57.5754	-58.5905	0.2500	0.2592
BD	1.0857	21.3135	-33.2971	-62.5942	-61.1781	-61.5942	-62.6093	0.1793	0.6564
KD	0.9682	19.3296	-33.0784	-62.1568	-60.7407	-61.1568	-62.1719	0.2055	0.4883
UGD	0.0209	0.9584	-31.1634	-58.3267	-56.9106	-57.3267	-58.3418	0.2438	0.2855
UMD	13.0409	18.8169	-30.3138	-56.6276	-55.2115	-55.6276	-56.6427	0.2981	0.1119
UWD	0.0043	3.9880	-32.6164	-61.2328	-59.8167	-60.2328	-61.2478	0.2476	0.2689
UBIIID	0.0467	6.0730	-20.1829	-36.3658	-34.9497	-35.3658	-36.3808	0.4944	0.0007
UBXIID	0.1245	6.5090	-16.6940	-29.3880	-27.9719	-28.3880	-29.4031	0.5227	0.0002

Table 9: Numerical values for analyzing the recovery rates dataset.

Models	γ	λ	ℓ	AIC	BIC	CAIC	HQIC	KS	KSpv
PRKD	1.7351	2.7811	-61.0285	-118.0570	-113.6777	-117.8665	-116.3265	0.0697	0.9054
MORKD	0.9644	14.8963	-57.1185	-110.2370	-105.8577	-110.0466	-108.5066	0.0883	0.6826
ERKD	0.8510	7.3504	-59.3988	-114.7976	-110.4183	-114.6071	-113.0671	0.0968	0.5661
RKD	0.6646	-	8.7255	19.4510	21.6407	19.5135	20.3163	0.6170	0.0000
TLD	10.5281	-	-51.5544	-101.1088	-98.9191	-101.0463	-100.2435	0.1813	0.0261
APTLD	15.6210	0.1700	-53.6762	-103.3523	-98.9730	-103.1618	-101.6218	0.1191	0.3062
BD	12.8124	4.9074	-57.5742	-111.1485	-106.7692	-110.9580	-109.4180	0.1150	0.3467
KD	8.0824	7.7412	-58.8343	-113.6686	-109.2893	-113.4781	-111.9381	0.0994	0.5313
UGD	0.2798	3.8426	-46.0283	-88.0567	-83.6774	-87.8662	-86.3262	0.1923	0.0152
UMD	3.5635	0.9274	-46.0283	-88.0566	-83.6773	-87.8661	-86.3262	0.1927	0.0148
UWD	8.6582	2.2330	-53.9658	-103.9315	-99.5522	-103.7411	-102.2011	0.1305	0.2106
UBIIID	5.4520	2.0635	-53.7962	-103.5924	-99.2131	-103.4020	-101.8620	0.1296	0.2174
UBXIID	10.5869	2.3584	-54.6292	-105.2585	-100.8791	-105.0680	-103.5280	0.1245	0.2576

lower information criteria values, thereby demonstrating a better balance between model complexity and goodness-of-fit.

The results for the Recovery Rates dataset in Table 9 further confirm the flexibility of the PRKD. The proposed model produces the smallest KS statistic and the largest KS*pv*, indicating excellent agreement between the empirical and fitted distributions. Moreover, the PRKD achieves competitive information criteria values relative to all other considered models, thereby supporting its suitability for modelling recovery rate data bounded within the unit interval.

For the Insurance dataset in Table 10, the PRKD attains the smallest information criteria values among the competing distributions and simultaneously provides one of the best goodness-of-fit performances based on the KS statistic and associated p-value. Although the MORKD yields a very close fit, the PRKD slightly outperforms it across most evaluation criteria, confirming the advantage gained through the additional shape flexibility introduced by the proposed model.

To further assess the adequacy of the PRKD, the fitted PDF, CDF, P-P, and Q-Q plots are displayed in Figs. 3 - 6. The graphical assessments reveal strong agreement between the empirical observations and the fitted PRKD across all datasets. In particular, the Q-Q and P-P plots show that the empirical points closely follow the reference lines with only negligible deviations, thereby confirming the suitability and robustness of the proposed distribution for modelling diverse forms of bounded data.

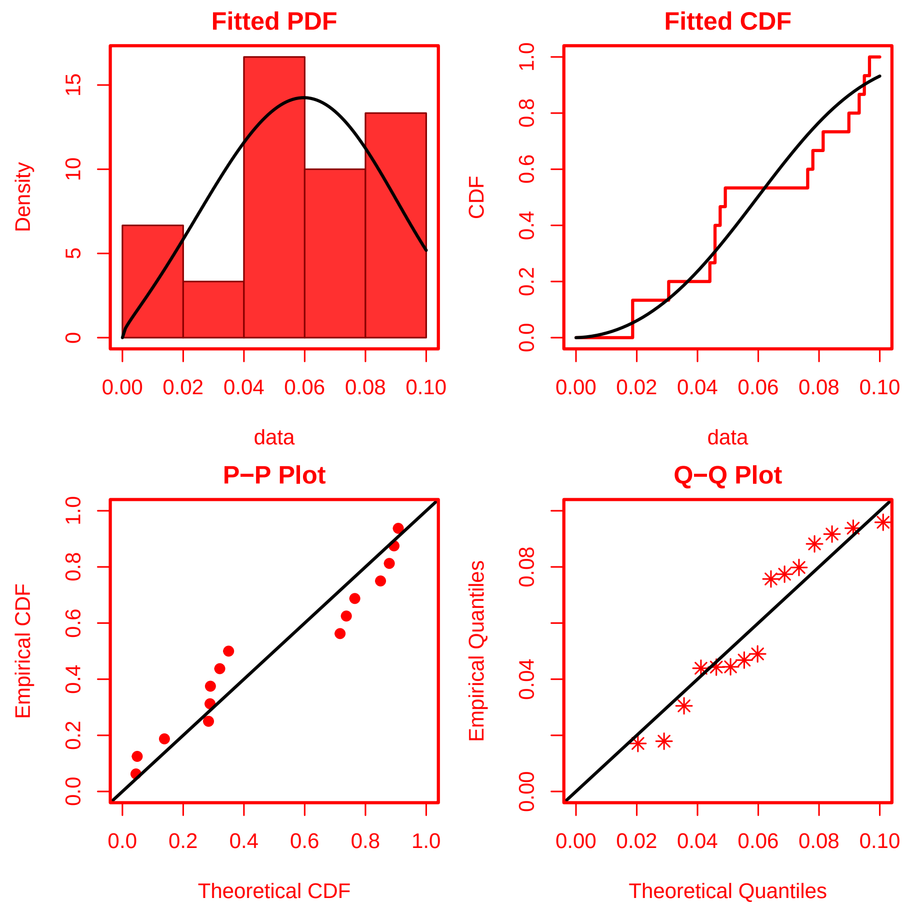

a

Figure 3: Fitted PDF, CDF, P-P and Q-Q plots of the PRKD for the PWP data.

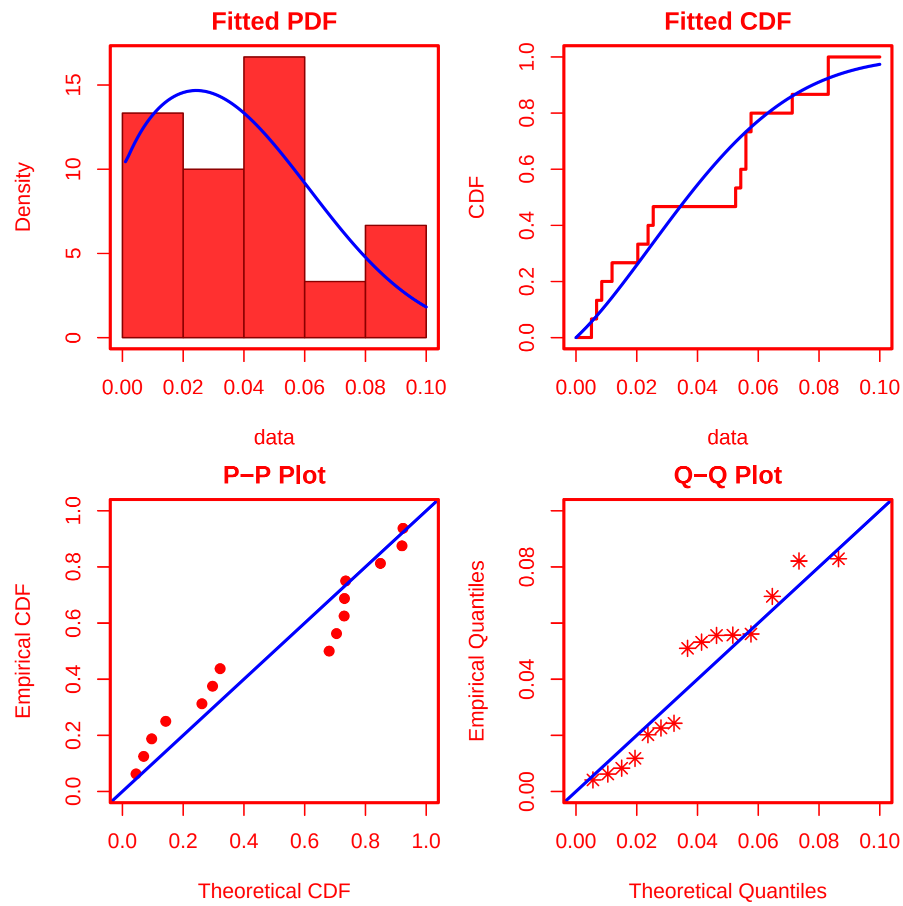

a

Figure 4: Fitted PDF, CDF, P-P and Q-Q plots of the PRKD for the soil moisture data.

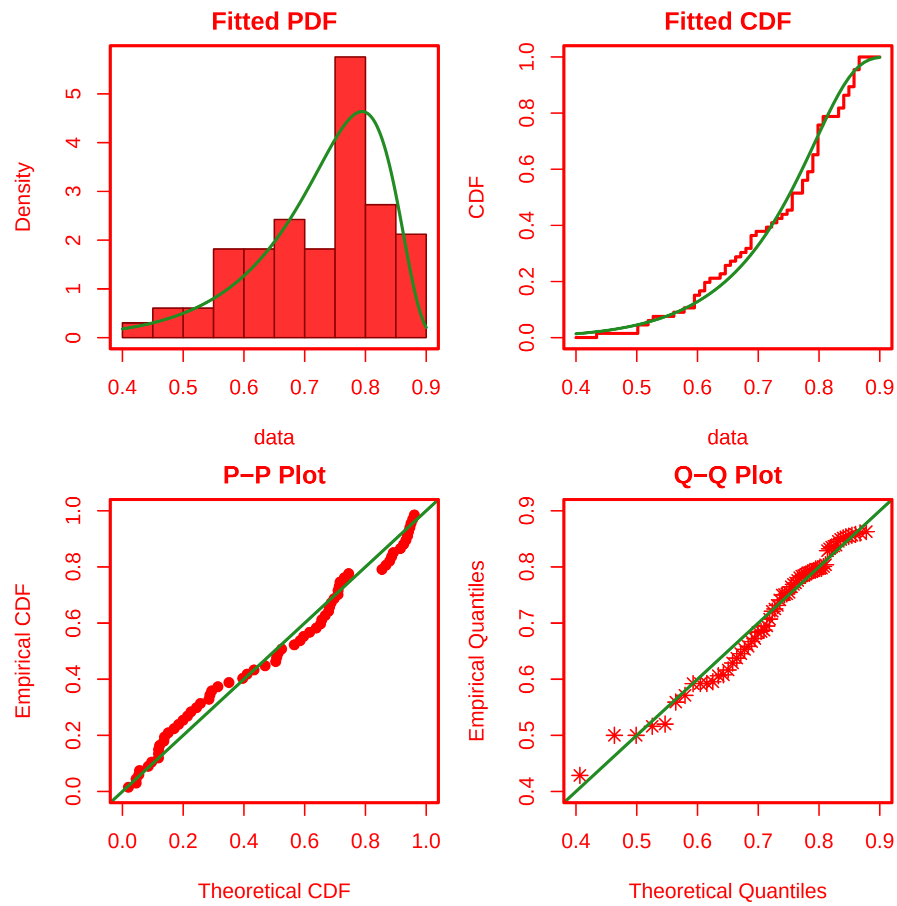

a

Figure 5: Fitted PDF, CDF, P-P and Q-Q plots of the PRKD for the recovery rates data.

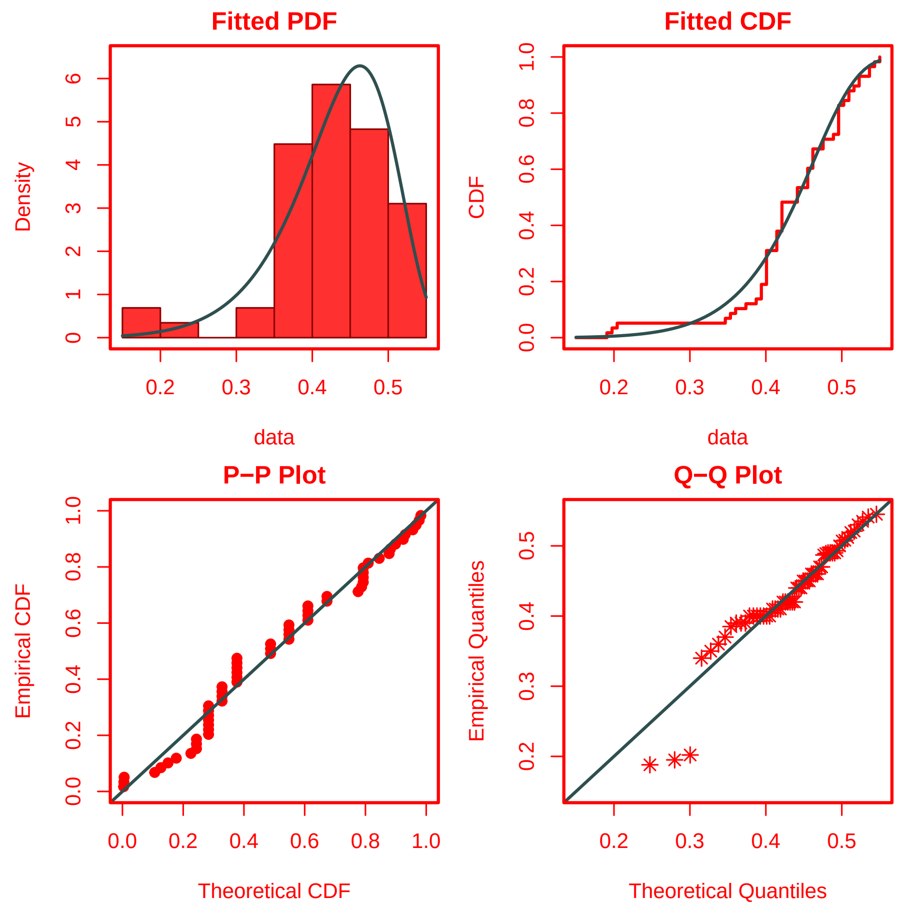

a

Figure 6: Fitted PDF, CDF, P-P and Q-Q plots of the PRKD for the insurance data.

Table 11 reports the likelihood ratio test (LRT) comparing PRKD against its baseline RKD, testing $H_0 : \lambda = 1$ versus $H_1 : \lambda \neq 1$. Across all four datasets, the LRT statistics were substantial and the associated p-values fell well below 0.05, leading to rejection of the null hypothesis throughout. This consistently indicates that the additional shape parameter λ contributes meaningfully to model flexibility, providing strong statistical evidence that PRKD offers a significantly better fit than RKD for each dataset examined.

Thus, the analytical and graphical findings collectively demonstrate that the PRKD provides a highly competitive and flexible modelling tool capable of accommodating varying degrees of skewness, kurtosis, and tail behaviour observed in practical unit interval datasets across various disciplines.

7 Conclusions

This study proposed the Power Reduced Kies distribution as a new and flexible two-parameter model for analysing bounded continuous data on the unit interval. The distribution was developed through a power transformation of the Reduced Kies distribution and was shown to possess considerable modelling flexibility through its diverse density and hazard rate shapes. Important structural and statistical properties of the distribution, including its linear representation, reliability characteristics, quantile function, ordinary moments, moment generating function, mode, and order statistics, were successfully derived in closed or tractable forms. The parameters of the PRKD were estimated using the maximum likelihood and maximum product of spacings methods. The Monte Carlo simulation study demonstrated that both estimation procedures perform satisfactorily and improve with increasing sample size. However, the maximum product of spacings estimator generally exhibited smaller mean squared errors and more stable finite-sample performance, particularly under smaller sample settings.

The applicability of the PRKD was further illustrated using four real datasets from environmental, insurance, and health-related studies. Comparative analyses with twelve competing unit distributions showed that the PRKD consistently provided superior or highly competitive fits according to several information criteria and goodness-of-fit measures. The graphical assessments also confirmed the adequacy of the proposed model in capturing the underlying data structures. Therefore, the PRKD constitutes a useful addition to the family of bounded distributions and offers a flexible alternative for modelling skewed and heterogeneous unit interval data encountered in several applied disciplines. Future research may consider the development of regression extensions, multivariate generalisations, Bayesian estimation procedures, and applications under censoring schemes and survival modelling structures.

Acknowledgement: The authors acknowledge the support of the Department of Statistics, Ahmadu Bello University, Zaria Nigeria, for providing the enabling environment to carry out this study.

Funding Statement: The author received no specific funding for this study.

Data Availability Statement: All data are provided within the article

Ethics Approval: Not applicable.

Use of Generative-AI tools declaration: The authors declare that no Artificial Intelligence (AI) tools were used in the creation of this article.

Conflicts of Interest: The author declares no competing interests

References

1. D. H. Abdelhady and Y. M. Amer, On the inverse power Gompertz distribution, *Annals of Data Science 8* **(2021)**, 451–473. https://doi.org/10.1007/s40745-020-00246-4
2. A. Z. Afify, M. Nassar, D. Kumar and G. M. Cordeiro, A new unit distribution: Properties, inference, and applications, *Electronic Journal of Applied Statistical Analysis 15* **(2022)**, 460–484. https://doi.org/10.1285/i20705948v15n2p460
3. M. A. Almuqrin, A. M. Gemeay, M. A. El-Raouf, M. Kilai, R. Aldallal and E. Hussam, A flexible extension of reduced Kies distribution: Properties, inference, and applications in biology, *Complexity 2022* **(2022)**, Article 6078567. https://doi.org/10.1155/2022/6078567
4. N. Alsadat, C. Taniş, L. P. Sapkota, C. S. Rajitha, M. M. Bahloul and A. M. Gemeay, Power unit exponential probability distribution: Statistical inference and applications, *Alexandria Engineering Journal 107* **(2024)**, 332–346. https://doi.org/10.1016/j.aej.2024.07.038

5. H. S. Bakouch, T. Hussain, M. Tošić, V. S. Stojanović and N. Qarmalah, Unit exponential probability distribution: Characterization and applications in environmental and engineering data modeling, *Mathematics 11* **(2023)**, 4207. https://doi.org/10.3390/math11194207
6. S. Bashir, B. Masood, L. A. Al-Essa, A. Sanaullah and I. Saleem, Properties, quantile regression, and application of bounded exponentiated Weibull distribution to COVID-19 data of mortality and survival rates, *Scientific Reports 14* **(2024)**, 1–17. https://doi.org/10.1038/s41598-024-65057-6
7. T. Bayes, An essay towards solving a problem in the doctrine of chances, *Philosophical Transactions of the Royal Society of London 53* **(1763)**, 370–418. https://doi.org/10.1098/rstl.1763.0053
8. J. C. Ehiwario, J. N. Igabari and P. E. Ezimadu, The alpha power Topp-Leone distribution: Properties, simulations and applications, *Journal of Applied Mathematics and Physics 11* **(2023)**, 316–331. https://doi.org/10.4236/jamp.2023.111020
9. E. E. Ehizojie, The exponentiated generalized reduced Kies distribution with properties and applications on Burr measurement datasets, *Malaysian Journal of Science and Advanced Technology 5* **(2025)**, 320–331. https://doi.org/10.56532/mjsat.v5i4.542
10. E. E. Ehizojie, The alpha power reduced Kies distribution: Properties, estimation techniques, and applications to insurance and dairy datasets, *Journal of Statistical Sciences and Computational Intelligence 2* **(2026)**, 406–423. https://doi.org/10.64497/jssci.272
11. A. M. Gemeay, N. Alsadat, C. Chesneau and M. Elgarhy, Power unit inverse Lindley distribution with different measures of uncertainty, estimation and applications, *AIMS Mathematics 9* **(2024)**, 20976–21024. https://doi.org/10.3934/math.20241021
12. A. M. Gemeay, A. Ezzebsa, H. Zeghdoudi, C. Tanış, Y. A. Tashkandy, M. E. Bakr and A. Kumar, The power new XLindley distribution: Statistical inference, fuzzy reliability, and applications, *Heliyon 10* **(2024)**, Article e36594. https://doi.org/10.1016/j.heliyon.2024.e36594
13. H. Haj Ahmad, E. M. Almetwally, M. Elgarhy and D. A. Ramadan, On unit exponential Pareto distribution for modeling the recovery rate of COVID-19, *Processes 11* **(2023)**, 232. https://doi.org/10.3390/pr11010232
14. I. Haruna, Y. Zakari, U. K. Abdullahi, R. O. David and J. Y. Falgore, On the study of Kumaraswamy reduced Kies distribution: Properties and applications, *Communications in Physical Sciences 12* **(2025)**, 1036–1060. https://doi.org/10.4314/cps.v12i2.15
15. A. S. Hassan, A. I. Al-Omar, D. M. Ismail and A. Al-Anzi, A new generalization of the inverse Lomax distribution with statistical properties and applications, *International Journal of Advanced and Applied Sciences 8* **(2021)**, 89–97. https://doi.org/10.21833/ijaas.2021.04.011
16. A. S. Hassan, S. M. Assar and A. M. Abdelghaffar, Statistical properties and estimation of power-transmuted inverse Rayleigh distribution, *Statistics in Transition New Series 21* **(2020)**, 93–107. https://doi.org/10.21307/stattrans-2020-046
17. E. Hussam, R. A. Aldallal, L. P. Sapkota and A. M. Gemeay, A modified half-logistic distribution with regression analysis, *Engineering Reports 7* **(2025)**, e70487. https://doi.org/10.1002/eng2.70487
18. A. Kies, The strength of glass, *Naval Research Laboratory*, Research Report, **1958**.
19. M. Ç. Korkmaz and C. Chesneau, On the unit Burr-XII distribution with the quantile regression modeling and applications, *Computational and Applied Mathematics 40* **(2021)**, 29. https://doi.org/10.1007/s40314-020-01341-0
20. M. Ç. Korkmaz and Z. S. Korkmaz, The unit log–log distribution: A new unit distribution with alternative quantile regression modeling and educational measurements applications, *Journal of Applied Statistics 50* **(2023)**, 889–908. https://doi.org/10.1080/02664763.2021.2001442
21. C. S. Kumar and S. H. S. Dharmaja, On reduced Kies distribution, In *Collection of Recent Statistical Methods and Applications*, C. S. Kumar, M. Chacko and E. I. A. Sathar (Eds.), *Univ. Kerala*, Dept. of Statistics, **2013**, pp. 111–123.

22. C. S. Kumar and S. H. S. Dharmaja, The exponentiated reduced Kies distribution: Properties and applications, *Communications in Statistics - Theory and Methods 46* **(2017)**, 8778–8790. https://doi.org/10.1080/03610926.2016.1183786
23. P. Kumaraswamy, A generalized probability density function for double-bounded random processes, *Journal of Hydrology 46* **(1980)**, 79–88.
24. R. Maiti, *Statistical Methods in Hydrology and Hydroclimatology*, *Springer*, Singapore, **2018**.
25. P. R. D. Marinho, R. B. Silva, M. Bourguignon, G. M. Cordeiro and S. Nadarajah, AdequacyModel: An R package for probability distributions and general purpose optimization, *PLoS ONE 14* **(2019)**, e0221487. https://doi.org/10.1371/journal.pone.0221487
26. R. Maya, P. Jodrá, M. R. Irshad and A. Krishna, The unit Muth distribution: Statistical properties and applications, *Ricerche di Matematica* **(2022)**. https://doi.org/10.1007/s11587-022-00703-7
27. J. Mazucheli, A. F. Menezes and S. Dey, Unit-Gompertz distribution with applications, *Statistica 79* **(2019)**, 25–43.
28. J. Mazucheli, A. F. B. Menezes and M. E. Ghitany, The unit-Weibull distribution and associated inference, *Journal of Applied Probability and Statistics 13* **(2018)**, 1–22.
29. K. Modi and V. Gill, Unit Burr-III distribution with application, *Journal of Statistics and Management Systems 23* **(2019)**, 823–838. https://doi.org/10.1080/09720510.2019.1646503
30. A. Saboor, F. Jamal, S. Shafq and R. Mumtaz, On the versatility of the unit logistic exponential distribution: Capturing bathtub, upside-down bathtub, and monotonic hazard rates, *Innovation in Statistics and Probability 1* **(2025)**, 28–46.
31. Y. A. Tashkandy, M. E. Bakr, S. A. Benchiha, L. P. Sapkota, O. S. Balogun, G. T. Mekiso, E. Hussam and A. M. Gemeay, Power modified XLindley distribution: Statistical properties and applications, *Scientific Reports 14* **(2024)**, Article 20262. https://doi.org/10.1038/s41598-024-69884-5
32. C. W. Topp and F. C. Leone, A family of J-shaped frequency functions, *Journal of the American Statistical Association 50* **(1955)**, 209–219.
33. A. Usman, G. S. S. Abdalla, E. E. Ehizojie and Y. Aliyu, Log-inverse Gompertz distribution with properties and applications to soil moisture and insurance datasets, *Computational Journal of Mathematical and Statistical Sciences 4* **(2025)**, 646–663. https://doi.org/10.21608/cjmss.2025.380747.1175
34. R. M. Usman, M. I. M. Usman and M. Ilyass, The power Burr Type X distribution: Properties, regression modeling and applications, *Punjab University Journal of Mathematics 52* **(2020)**, 27–44.
35. E. Yıldırım, E. S. Ilıkkan, A. M. Gemeay, N. Makumi, M. E. Bakr and O. S. Balogun, Power unit Burr-XII distribution: Statistical inference with applications, *AIP Advances 13* **(2023)**, Article 105107. https://doi.org/10.1063/5.0171077

Table 10: Numerical values for analyzing the insurance dataset.

Models	γ	λ	ℓ	AIC	BIC	CAIC	HQIC	KS	KSpv
PRKD	4.3982	0.9012	-74.5207	-145.0414	-140.9205	-144.8232	-143.4363	0.1058	0.5350
MORKD	5.1533	0.3451	-73.7209	-143.4417	-139.3208	-143.2235	-141.8366	0.1059	0.5331
ERKD	7.0598	0.4473	-74.3079	-144.6158	-140.4949	-144.3976	-143.0106	0.1300	0.2808
RKD	3.9685	-	-65.6545	-129.3089	-127.2485	-129.2375	-128.5063	0.2615	0.0007
TLD	2.4396	-	-24.4158	-46.8316	-44.7711	-46.7602	-46.0290	0.4322	0.0000
APTLD	6.2380	0.0007	-59.7683	-115.5367	-111.4158	-115.3185	-113.9315	0.1902	0.0301
BD	16.2839	21.5508	-65.5101	-127.0201	-122.8993	-126.8020	-125.4150	0.1749	0.0576
KD	4.6268	34.0335	-64.0837	-124.1674	-120.0465	-123.9492	-122.5622	0.2180	0.0081
UGD	0.0656	2.8804	-38.4004	-72.8008	-68.6799	-72.5826	-71.1956	0.2676	0.0005
UMD	15.1993	5.2856	-38.4007	-72.8013	-68.6805	-72.5832	-71.1962	0.2673	0.0005
UWD	1.2432	3.6249	-52.0349	-100.0697	-95.9488	-99.8515	-98.4646	0.2301	0.0043
UBIIID	0.2586	12.3988	-73.6403	-143.2807	-139.1598	-143.0625	-141.6755	0.1292	0.2875
UBXIID	2.2484	6.2680	-65.4318	-126.8635	-122.7426	-126.6454	-125.2584	0.1711	0.0670

Table 11: Table 11: The likelihood ratio test for the datasets.

Dataset	LogLik RKD	LogLik PRKD	LRT Statistic	Degree of Freedom	p-value
PWP	- 9.4758	- 33.6449	48.3384	1	3.587×10^{-12}
Soil Moisture	- 15.2868	- 34.7801	38.9866	1	4.267×10^{-10}
Recovery Rates	8.7255	- 61.0285	139.508	1	0
Insurance	- 65.6545	- 74.5207	17.7325	1	2.542×10^{-9}